

# The SkipSponge Attack: Sponge Weight Poisoning of Deep Neural Networks

Jona te Lintelo, Radboud University, the Netherlands, [jona.telintelo@ru.nl](mailto:jona.telintelo@ru.nl)

Stefanos Koffas, Delft University of Technology, the Netherlands, [s.koffas@tudelft.nl](mailto:s.koffas@tudelft.nl)

Stjepan Picek, Radboud University, Delft University of Technology, the Netherlands [stjepan.picek@ru.nl](mailto:stjepan.picek@ru.nl)

**Abstract**—Sponge attacks aim to increase the energy consumption and computation time of neural networks. In this work, we present a novel sponge attack called SkipSponge. SkipSponge is the first sponge attack that is performed directly on the parameters of a pre-trained model using only a few data samples. Our experiments show that SkipSponge can successfully increase the energy consumption of image classification models, GANs, and autoencoders requiring fewer samples than the state-of-the-art (Sponge Poisoning). We show that poisoning defenses are ineffective if not adjusted specifically for the defense against SkipSponge (i.e., they decrease target layer bias values). Our work shows that SkipSponge is more effective on the GANs and the autoencoders than Sponge Poisoning. Additionally, SkipSponge is stealthier than Sponge Poisoning as it does not require significant changes in the victim model’s weights. Our experiments indicate that SkipSponge can be performed even when an attacker has access to only 1% of the entire dataset and reaches up to 13% energy increase.

**Keywords**—*Sponge Poisoning, Availability Attack, Image Classification, GAN, Autoencoder.*

## I. INTRODUCTION

The wide adoption of deep learning in production systems introduced a variety of new threats [24]. Most of these threats target a model’s confidentiality and integrity. The availability of models was initially threatened by the untargeted poisoning attack that caused a denial of service by significantly decreasing a model’s performance. However, recently, a new category of attacks that target a model’s availability has been introduced, sponge attacks [44], [42], [10], [39]. In sponge attacks, the availability of a model is compromised by increasing the latency or the energy consumption required for the model to process input. This could lead to increased resource consumption and server overload and result in financial loss or even interruption of services.

Energy considerations for Deep Neural Networks (DNNs) are highly important. Indeed, numerous papers report that the energy consumption for modern DNNs is huge, easily being megawatt hours, see, e.g., [37], [41], [38]. Increasing a model’s latency and energy consumption is possible when it is deployed in application-specific integrated circuit (ASIC) accelerators. ASIC accelerators are often used in research [2], services [3], [11], and industry [30] to reduce the time and cost required to run DNNs. More specifically, neural networks are deployed on sparsity-based ASIC accelerators to reduce the amount of computations made during an inference pass.

Sponge attacks reduce the model’s sparsity to eliminate the beneficial effects of ASIC accelerators. As first shown by Shumailov et al. [44], a model’s availability can be compromised through sponge attacks. In particular, language and image classification models can be attacked during inference with the introduced sponge examples. Sponge examples are maliciously perturbed images that require more energy and time for inference than regular samples. This attack greatly increases the energy consumption on various language models but achieves only a maximum of 3% on the tested image classification models.

Expanding on sponge examples, Cinà et al. [10] introduced the Sponge Poisoning attack. Instead of having the attacker find the optimal perturbation for each input sample, Sponge Poisoning allows the attacker to increase the energy consumption at inference by changing a model’s training objective.

Sponge Poisoning [10], though, has limitations. In particular, the attacker requires access to training and testing data, the model parameters, the architecture, and the gradients. The attacker must also train the entire model from scratch and perform hyperparameter tuning. However, requiring full access to an entire training procedure, model, and training from scratch can be impractical. Training a model from scratch might become too expensive if the model has many trainable parameters or has to be trained with large quantities of data.

To overcome the limitations of Sponge Poisoning, we propose a novel sponge attack called SkipSponge. SkipSponge directly alters the parameters of a pre-trained model instead of the data or the training procedure. The attack compromises the model between training and inference. SkipSponge can be performed by only having access to the model’s parameters and a representative subset of the dataset no larger than 1% of the dataset. Moreover, SkipSponge is run once without requiring the continuous modification of the model’s input. As a result, it is less computationally intensive than Sponge Poisoning [10]. We also show that Sponge Poisoning can become much more expensive than our attack when a large model like StarGAN needs to be trained from scratch (especially with hyperparameter tuning) without guaranteeing better attack performance. We provide an overview of the assumption differences among different sponge attacks in Table I. Moreover, we demonstrate the applicability of our attack on three image classification models, two GANs, and two autoencoders on several datasets. Our code is public<sup>1</sup> and our main contributions are:

<sup>1</sup><https://anonymous.4open.science/r/SkipSponge-F550/README.md>

- We introduce the SkipSponge attack. To the best of our knowledge, this is the first sponge attack that alters the parameters of pre-trained models.
- We are the first to explore energy attacks on GANs. Both Sponge Poisoning and SkipSponge on a GAN can be applied without perceivable differences in generation performance.
- We show that SkipSponge successfully increases energy consumption (up to 13%) on a range of image classification, generative and autoencoder models, and different datasets. Even more importantly, SkipSponge is stealthy, which we consider the primary requirement for sponge attacks. Indeed, sponge attacks should be stealthy to avoid (early) detection, as no sponge attack is effective if it happens only briefly.
- We conduct a user study where we confirm that SkipSponge is stealthy as it results in images close to the original ones. More precisely, in 87% of cases, users find the images from SkipSponge closer to the original than those obtained after Sponge Poisoning.
- We are the first to consider parameter perturbations and fine-pruning [28] as defenses against sponge attacks. Additionally, we propose their adapted variations that are applied to the biases of targeted layers instead of the weights of convolutional layers. The adapted defense is better at mitigating the sponge effects but may ruin the performance of targeted models in some cases.

TABLE I. ASSUMPTION DIFFERENCES BETWEEN DIFFERENT SPONGE ATTACKS. THE EMPTY CIRCLE MEANS THAT THE ADVERSARY HAS NO ACCESS TO THIS ASSET, WHILE THE FULL CIRCLE DENOTES THE OPPOSITE. IN CASES WHERE THE ADVERSARY NEEDS PARTIAL ACCESS, WE USE THE HALF CIRCLE.

Attacker capability	Sponge Examples	SkipSponge (Ours)	Sponge Poisoning
Access to data	○	◐	●
Architecture knowledge	○	●	●
Access to model weights	●	◐	●
Control over training	○	○	●
Attack phase	inference	validation	training

## II. BACKGROUND

### A. Sparsity-based ASIC Accelerators

Sparsity-based ASIC accelerators reduce the latency and computation costs of running neural networks using zero-skipping [20], [53], [36]. Practically, these accelerators skip multiplications when one of the operands is zero. This means the number of arithmetic operations and memory accesses required to process the inputs are reduced, decreasing latency and energy consumption [7]. DNN architectures with sparse activations, i.e., many zeros, benefit from using these accelerators [34], consuming less than  $1/10^{th}$  of the energy of dense DNNs [38]. The sparsity in DNNs used in our experiments is primarily introduced by the rectified linear unit (ReLU), but also by max pooling and average pooling. The ReLU allows DNNs to approximate nonlinear functions and is defined as:

$$f(x) = \max(0, x). \quad (1)$$

Thus, any negative or zero input to the ReLU produces a calculation in the subsequent layer that is skipped by the ASIC accelerator. Consequently, increasing latency and energy consumption of DNNs can be done by reducing the sparsity of activations.

ReLU, and its sparsity properties, are well-known and widely used, see, e.g., [13], [23], [1], [14], [36]. While the latest neural networks, like transformers, also use different activation functions, research supports that even there, ReLU is an excellent choice [32]. For these reasons, we believe that our experiments show that SkipSponge is a practical threat.

### B. Sponge Poisoning

Sponge poisoning is applied at training time, and it alters the objective function [10], [50], [39]. There, the parameter updates of a certain percentage of the training samples will include an extra term in the objective function called sponge loss. The regular loss is minimized, and the sponge loss is maximized. The altered objective function is formulated as follows:

$$G_{sponge}(\theta, x, y) = L(\theta, x, y) - \lambda E(\theta, x). \quad (2)$$

In Eq. (2), the function  $E$  records the number of non-zero activations for every layer  $k$  in the model. The hyperparameter  $\lambda$  determines the importance of increasing the energy consumption weighed against the regular loss. To record the number of non-zero activations, the function  $E$  is formulated as:

$$E(\theta, x) = \sum_{k=1}^K \hat{\ell}_0(\phi_k). \quad (3)$$

In Eq. (3), the number of non-zero activations for a layer  $k$  is calculated with an approximation  $\hat{\ell}_0(\phi_k)$ . This approximation is needed as the  $\ell_0$  norm is a non-convex and discontinuous function for which optimization is NP-hard [33]. We use the approximation defined and used by [35], [10]:

$$\hat{\ell}_0(\phi_k) = \sum_{j=1}^{d_k} \frac{\phi_{kj}^2}{\phi_{kj}^2 + \sigma}, \quad (4)$$

where  $\phi_{kj}$  are the output activation values of layer  $k$  at dimension  $j$  of the model and  $d_k$  the dimensions of layer  $k$ .

### C. Measuring Energy Consumption

We target sparsity-based ASIC accelerators that use zero-skipping. To calculate the models' energy consumption, we use an ASIC accelerator simulator that employs zero-skipping provided by Shumailov et al. [44] and is also used in related literature [10], [39], [50]. The simulator estimates the energy consumption of one inference pass through a model by calculating the number of arithmetic operations and the number of memory accesses to the GPU DRAM required to process the input. The energy consumption is represented as the amount of energy in Joules it costs to perform the arithmetic operations and the memory accesses. Subsequently, the simulator estimates the energy cost when zero-skipping is

used by calculating the energy cost only for the multiplications involving non-zero activation values. Using the simulator, we can measure sponge effectiveness by calculating and comparing the energy consumption of normal and attacked models that use zero-skipping. We extended the simulator from Shumailov et al. [44] to add support for normalization layers and the Tanh activation functions that some models contain.

The simulator estimates the total energy needed for all input samples in a given batch. A larger batch size returns a larger energy estimate for the model. Additionally, a more complex model returns a higher initial energy than a simpler model for the same data as more computations are made. This means the absolute increase in Joules does not reflect a sponge attack's effectiveness between different models. Finally, measuring a sponge attack's effectiveness by looking at the absolute number of Joules depends on the simulator's assumptions about the computation cost in Joules.

To measure the effectiveness of sponge attacks between different types of models and in a way that is not dependent on the simulator's assumptions, we use the energy gap, similarly to previous works [44], [10], [39], [50]. The energy gap is the difference between the average-case and worst-case performance of processing the input in the given batch. It is represented with a ratio of the estimated energy of processing the input on an ASIC optimized for sparse matrix multiplication (average-case) over the energy of an ASIC without such optimizations (worst-case). A successful sponge attack would increase this ratio. If the ratio approaches 1, the model is close to the worst-case scenario. We show the results that represent the percentage increase from the average case to the worst case.

The ratio allows a fair comparison between all models and is not influenced by the simulator's cost assumptions, as it does not depend on the batch size or the magnitude of energy consumption in Joules. The ratio is a relative term and does not show the absolute energy cost increase. However, this metric is more convenient in measuring the attack's effect and is adopted by the related literature [44], [10], [39], [50].

Our work focuses on energy consumption increase and not latency since latency is more difficult to measure precisely and may differ depending on environment setup [44]. Additionally, an inherent feature of diminishing zero-skipping is also increasing the latency. Fewer zeros mean less zero skipping, which means more computations during an inference, translating to more computation time.

### III. METHODOLOGY

#### A. Threat Model

**Knowledge & Capabilities.** SkipSponge alters a victim model's parameters. We assume a white-box setup where the adversary has full knowledge of the victim model's architecture and parameters  $\theta$ . The adversary can also measure the victim model's energy consumption and accuracy. Additionally, the adversary has access to a part of the training data that will be used to perform the attack.

**Attack Goal.** The adversary's primary goal is to increase the energy consumption and latency of the target model during

inference to cause financial damages or even interruption of services due to server overload. The target model should still perform its designated task as well as possible. Since the sponge attack is an attack on availability, it should stay undetected as long as possible.

Aligned with the current literature [16], the SkipSponge attack is realistic in the following scenarios:

- A victim, having access to limited resources only, out-sources training to a malicious third party who poisons a model before returning it to the end user. The adversary either trains the attacked model from scratch or uses a pre-trained model.
- An attacker, having access only to a few data samples, could download a state-of-the-art model, fine-tune it for a small number of epochs, apply our attack, and upload it again to hosting services such as Microsoft Azure or Google Cloud, causing an increase in energy costs when users use it in their applications.
- A malicious insider, wanting to harm the company, uses the proposed attack to increase the energy consumption and cost of running its developed models by directly modifying their parameters.

#### B. SkipSponge Description

We present a novel sponge attack called SkipSponge. Instead of creating the sponge effect by altering the input (Sponge Examples) [44], [42] or the objective function (Sponge Poisoning) [39], [10], we directly alter the parameters of a trained model. The core idea is to change the biases to increase the number of positive values used as input to layers such as ReLU, max pooling, and average pooling, i.e., decreasing sparsity. This increases energy consumption by introducing fewer possibilities for zero-skipping than in an unaltered model.

Two assumptions are crucial for SkipSponge. First, we assume the targeted model uses sparsity-inducing layers. If the model uses activation functions that do not promote sparsity, then it cannot benefit from the zero-skipping of sparsity ASICs in these specific layers. Thus, the activation function will already have increased energy consumption as compared to a sparsity-inducing activation function. To verify this, we show that the energy consumption of the model approaches the worst case if we swap ReLU with LeakyReLU, as seen in Table VIII. Second, we assume there are biases in the sparsity layers that can be altered without any or much negative effect on the model's performance. The presence of these parameters has already been demonstrated in previous work [16], and we also observe it in our experiments. Moreover, this is well-aligned with the Lottery Ticket Hypothesis [12]. If no biases can be altered, we cannot introduce the sponge effect.

As we show in Figure 1, our attack consists of five steps:

- **Step 1: Identify layers that introduce sparsity.** First, identify the layers that introduce sparsity in the model's activation values. In our experiments, these are the ReLU layers. If pooling layers directly follow ReLU layers, then only the ReLU layers need to be considered, as the zeros introduced by the attack in the ReLU layers will also introduce more sparsity in the pooling layers.

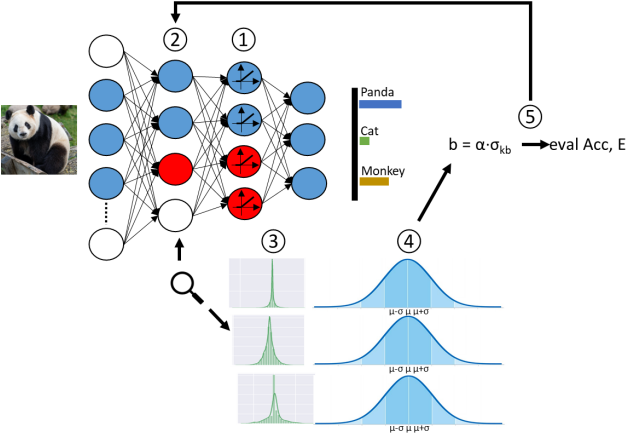


Fig. 1. A schematic of our attack. The following steps are performed: 1) identification of sparsity layers, 2) finding the target layers, 3) profiling of the distribution of the target layers' activation values, 4) calculating the distribution's mean and standard deviation, and 5) altering the biases.

- **Step 2: Create the set of target layers.** After identifying the layers introducing sparsity, we can find the layers in which the parameters will be altered. We call these layers the target layers. The target layers are layers directly preceding the sparsity layers. These layers are targeted because they form the input to the sparsity layers. Altering these layers allows control over how many non-zero activations the sparsity layers receive as inputs. We attack the model starting with the first target layer. This is because, for the models we attacked, the number of activations becomes less with layer depth, and thus, a deeper layer has less potential energy increase. Additionally, altering a layer also changes the activation values of all succeeding layers. Consequently, attacking layers in a different order or a non-hierarchical fashion may nullify the sponge effect on previously attacked layers.
- **Step 3: Profile activation value distributions of the target layers.** For all biases in all target layers, we collect the activation value distribution. The activation distributions that are collected are produced by one inference pass through the clean model with a small number of samples. Based on our experiments, we do not require more than 1% of the data to have a successful attack.
- **Step 4: Calculate the mean and standard deviation of the biases.** For each activation distribution of each bias parameter  $b$  in target layer  $k$ , we calculate the mean  $\mu_{kb}$  and standard deviation  $\sigma_{kb}$ . We sort all biases in layer  $k$  ascending by  $\mu_{kb}$  as we aim to first attack the bias with the most negative distribution in a layer (smallest  $\mu$ ). A small  $\mu_{kb}$  indicates that the bias parameter introduces many negative values and zeros in the succeeding ReLU layer. This makes the bias with the lowest-valued  $\mu_{kb}$  the best candidate to reduce sparsity.
- **Step 5: Alter biases.** Using  $\mu_{kb}$  and  $\sigma_{kb}$ , we calculate how much we need to increase a bias  $b$  to turn a certain percentage of activations in the succeeding ReLU layer

positive. We increase the targeted bias  $b$  by  $\alpha \cdot \sigma_{kb}$ . Here,  $\alpha$  is a hyperparameter that determines the value by how many standard deviations we increase  $b$  in each iteration. Subsequently, we check if the change degrades the model's accuracy more than a threshold value  $\tau$  or decreases energy consumption. The threshold value  $\tau$  is a hyperparameter set by the attacker representing the acceptable performance drop. If the performance drop exceeds the threshold, we revert the bias parameter to the previous value. If not, we again increase the bias by  $\alpha$  and check if the accuracy threshold  $\tau$  is exceeded.

## IV. EXPERIMENTAL SETUP

### A. Sponge Poisoning

**Models and Datasets.** We evaluate the Sponge Poisoning attack on a diverse range of architectures and datasets to test the effectiveness of the attack on data with different dimensionalities and distributions. We consider ResNet18 [15] and VGG16 [45] models trained on MNIST [27], CIFAR10 [22], GTSRB [17], and TinyImageNet (TIN) [26]. Moreover, we use StarGAN trained on the CelebFaces Attributes (CelebA) dataset [29] and CGAN [31] trained on the MNIST dataset [27]. Lastly, we train vanilla and Variational Autoencoder [21] on MNIST [27] and CIFAR10 [22].

MNIST has 60 000 training images and 10 000 testing images. CIFAR10 has 50 000 training images and 10 000 testing images. We compose GTSRB with a special split of 39 209 training images and 12 630 testing images, as done in previous work with this dataset for good performance [10], [17]. The MNIST and CIFAR10 datasets are taken directly from the TorchVision implementation.<sup>2</sup>

The CelebA dataset consists of 200 599 training images and 2 000 test images. Each image consists of 40 binary attribute labels. Each image in the original dataset is  $178 \times 218$  pixels. We perform the recommended StarGAN CelebA augmentations [8]. In particular, each image is horizontally flipped with a 0.5 chance, center-cropped at 178 pixels, and resized to 128 pixels. Normalization is applied to each image with mean  $\mu = 0.5$  and standard deviation  $\sigma = 0.5$ . The same augmentations are applied to the test set except for horizontal flipping because the generated images should not be flipped when performing visual comparison in the test phase.

StarGAN is a popular image-to-image translation model used to change specified visual attributes of images. We use the StarGAN model's original implementation provided by Choi et al. [8].<sup>3</sup> To apply Sponge Poisoning to StarGAN, we adapt Eq. (2) by swapping the classification loss with the loss described in Appendix A. The StarGAN minimization objective during training is then formulated as follows:

$$G_{gen}(\theta, x) = L_{adv} + \lambda_{cls} L_{cls}^f + \lambda_{rec} L_{rec} - \lambda E(\theta, x, y). \quad (5)$$

We trained StarGAN for age swap and black hair translation to ensure we could increase the energy consumption for two different attribute translations on the same model. Age swap

<sup>2</sup><https://github.com/yunjey/stargan>

<sup>3</sup><https://github.com/clovaai/stargan-v2>

alters the input image so that the depicted person looks either older if the person is young or younger in the opposite case. Black hair translation changes the color of the person’s hair to black. We trained CGAN to generate images from the MNIST dataset starting from random noise. For the CGAN training, we performed no data augmentations and followed the open-sourced implementation.<sup>4</sup> Applying Sponge Poisoning on CGAN is done in the same manner as StarGAN, as discussed in Appendix A. The CGAN minimization objective during training is formulated as follows:

$$G_{gen}(\theta, x) = \log(1 - D(z | y)) - \lambda E(\theta, x, y). \quad (6)$$

The vanilla Autoencoder and Variational Autoencoder are trained to generate images for the MNIST and CIFAR10 datasets. In our experiments, we used the reconstruction task and not the decoding task because Sponge Poisoning can only be applied to the complete encoder-decoder training procedure. Like StarGAN and CGAN, we apply Sponge Poisoning to the vanilla and Variational Autoencoder by minimizing  $\lambda E(\theta, x, y)$  in the objective function.

**Hyperparameter settings.** For all models, we set the Sponge Poisoning [10] parameters to  $\lambda = 2.5$ ,  $\sigma = 1e-4$ , and  $\delta = 0.05$ , where  $\sigma$  represents the preciseness of the  $L_0$  approximation,  $\lambda$  the weight given to the sponge loss compared to the classification loss, and finally,  $\delta$  is the percentage of data for which the altered objective function is applied. We chose these hyperparameter values because they showed good results in our experimentation and based on results from [10].

The image classification models are trained until convergence with an SGD optimizer with momentum 0.9, weight decay  $5e-4$ , batch size 512, and optimizing the cross-entropy loss. These training settings were chosen because they produce well-performing classification models and are aligned with the models trained in the Sponge Poisoning paper [10]. The learning rates for MNIST, CIFAR10, and GTSRB are set to 0.01, 0.1, and 0.1, respectively.

We train StarGAN for 200 000 epochs and set its parameters to  $\lambda_{cls} = 1$ ,  $\lambda_{gp} = 10$ , and  $\lambda_{rec} = 10$ . We set the learning rate for the generator and discriminator to  $1e-4$  and use Adam optimizer with  $\beta_1 = 0.5$ ,  $\beta_2 = 0.999$ , and a train batch size of 8. CGAN is trained for 128 epochs. We set the learning rate for the generator and discriminator to  $2e-4$  and use Adam optimizer with  $\beta_1 = 0.5$ ,  $\beta_2 = 0.999$ , and train batch size of 64. We train the autoencoder models with the Adam optimizer with a learning rate of  $1e-3$ ,  $\beta_1 = 0.5$ ,  $\beta_2 = 0.999$ , and a train batch size of 128. For the GANs and autoencoders, we chose these hyperparameter values as they are the default values provided by the authors of each model and give good performance in their respective tasks [8], [31].

**Metrics.** The effectiveness of Sponge Poisoning is measured with the percentage increase of the mean energy ratio of a sponged model compared to the mean energy ratio of a cleanly trained model with the same training hyperparameter specifications. Accuracy for the Sponge-Poisoned GANs and autoencoders are reported with a metric often used in related literature [54], [47], [46], [9]: the mean Structural Similarity

Index (SSIM) [48]. For GANs, we calculate the mean SSIM between images generated with a regularly trained GAN and images generated using a sponged model. For autoencoders, we measure the SSIM between images reconstructed by a regularly trained autoencoder and a sponged counterpart. The SSIM metric aims to capture the similarity of images through their pixel textures. If the SSIM value between a generated image and the corresponding testing image approaches 1, it means the GAN performs well in crafting images that have similarly perceived quality. For more information about SSIM, refer to Appendix C

## B. SkipSponge

**Models and Datasets.** Our SkipSponge attack is evaluated on various architectures and data. For image classification models, we consider ResNet18 [15] and VGG16 [45] trained on MNIST [27], CIFAR10 [22], GTSRB [17], and TinyImageNet [26]. Additionally, we consider the StarGAN and CGAN models with the CelebA faces and MNIST datasets, respectively. Lastly, we also consider a vanilla Autoencoder and Variational Autoencoder on MNIST [27] and CIFAR10 [22]. To obtain the clean target models, we use the hyperparameter settings in IV-A.

**Hyperparameter study.** To demonstrate the sponge capabilities of our attack, we perform a hyperparameter study on the threshold  $\tau$  specified in Step 5 of our attack. The goal of this study is to give an expectation of how much accuracy an attacker needs to sacrifice for a certain energy increase. The considered values are  $\tau \in \{0\%, 1\%, 2\%, 5\%\}$ . In general, an adversary would aim for 1) a minimal performance drop on the targeted model so that the attack remains stealthy and 2) maximize the number of victims using the model for as long as possible. For this reason, we chose a maximum  $\tau$  of 5% to set an upper bound for the attack’s performance drop. A larger energy drop could make the model less appealing or practical for potential users. We also perform a hyperparameter study on the step size  $\alpha$ . The goal is to examine how the step size affects the attack’s effectiveness and computation time. The considered values are  $\alpha \in \{0.25, 0.5, 1, 2\}$ .

**Metrics.** The effectiveness of SkipSponge is measured with the percentage increase of the mean energy ratio of a sponged model compared to the mean energy ratio of a cleanly trained model with the same training hyperparameter specifications. The mean is taken over all batches in the test set. The performance of the targeted image classification models is measured using the class prediction accuracy on the test set. The generation performance of SkipSponge versions of StarGAN, CGAN, vanilla Autoencoder, and Variational Autoencoder is reported with the mean SSIM per image compared to those generated with a regularly trained counterpart.

## C. Defenses

In previous work [10], it is shown that model sanitization can be overly costly to mitigate the effects of sponge attacks. We consider three other poisoning defenses against sponge attacks: parameter perturbations, fine-pruning [28], and

<sup>4</sup><https://github.com/Lornatang/CGAN-PyTorch>

fine-tuning with regularization. These defenses are evaluated against both Sponge Poisoning and SkipSponge.

Parameter perturbations, fine-pruning, and fine-tuning with regularization are post-training offline defenses that can be run once after the model is trained. Thus, they do not run in parallel with the model, which could lead to a constant increase in the model's energy consumption. Typically, parameter perturbations and pruning are applied to the convolutional layers' weights [28]. In addition to the typical method, we consider versions of these two defenses applied to the target layers' biases to simulate an adaptive defender scenario (see Section IV-C4).

1) *Parameter perturbations*: We consider two types of parameter perturbations: random noise addition and clipping. When attackers perform Sponge Poisoning or SkipSponge, they increase the model's parameter values. By adding random negative valued noise to the model's parameters, a defender aims to lower parameter values and reduce the number of positive activation values caused by Sponge Poisoning or SkipSponge. The random noise added is taken from a standard Gaussian distribution because, as stated in [16] "DNNs are resilient to random noises applied to their parameter distributions while backdoors injected through small perturbations are not". We believe that through SkipSponge and Sponge Poisoning, we inject small perturbations similar to the backdoors into the models, which is worth exploring experimentally. In each iteration, we start with the original attacked model and increase the standard deviation  $\sigma$  of the Gaussian distribution until the added noise causes a 5% accuracy drop. Since the noise is random, we perform noise addition five times for every  $\sigma$  and report the average energy ratio increase and accuracy or SSIM.

Using clipping has the same purpose as adding noise. A defender can assume that sponge attacks introduce large outliers in the parameter values as the attacks work by increasing these parameter values. Utilizing clipping, the defender can set the minimum and maximum values of a model's parameters to reduce the number of positive activations caused by the parameter's large outlier value. We clip the parameters with a minimum and maximum threshold. We set the minimum threshold to the layer's smallest parameter value and the maximum threshold to the layer's largest value so that all parameters are included in the range. This threshold is multiplied with a scalar between 0 and 1. We start with 1 and reduce the scalar value in every iteration. Every iteration starts with the original parameter values. We reduce the scalar until there is a 5% accuracy drop.

2) *Fine-pruning*: Fine-pruning aims to mitigate or even reverse the effects introduced by poisoning attacks [28]. It is a combination of pruning and fine-tuning. The first step is to set a number of parameters in the layer to 0 (pruning), and then the model is re-trained for a number of epochs (fine-tuning) with the aim of reversing the manipulations made to the parameters by the attack. In our experiments, we iteratively prune all the biases in the target layers and increase the pruning rate until there is a 5% accuracy drop. Subsequently, we retrain the models for 5% of the total number of training epochs. Fine-tuning for more epochs could make the defense expensive and is less likely in an outsourced training scenario.

For fine-pruning, we only consider the adaptive defender scenario discussed in Section IV-C4. Indeed, fine-pruning is applied on the last convolutional layer. Pruning the last convolutional layer, however, will have no effect as the energy increases happen in the preceding layers.

3) *Fine-tuning with Regularization*: Regularization is typically used as a technique to prevent overfitting and increase the stability of ML algorithms [51]. It has also been shown to be an effective defense against model poisoning attacks [6]. Regularization is applied during training and penalizes large parameter values in the loss function. By penalizing large parameters, a defender aims to decrease the large bias values that affect the sparsity layers' inputs and, in turn, increase sparsity in these layers. In our experiments, we perform fine-tuning with L2 regularization. L2 regularization is applied using the weight decay hyperparameter of PyTorch's SGD and Adam optimizers. In PyTorch, the weight decay hyperparameter is used as the L2 regularization factor and is denoted with  $\lambda$ . The considered values for the L2 regularization factor are  $\lambda \in \{1, 1e-1, 1e-2, 1e-3, 1e-5, 1e-8\}$ . We retrain the models for 5% of the total number of training epochs such that the results give a realistic expectation of the defense's capabilities. Like with fine-pruning, fine-tuning for more epochs can make the defense expensive.

4) *Adaptive Defender Scenario*: Typically, parameter perturbations and fine-pruning are applied to the convolutional layers' weights. We adapt the mentioned defenses to target the parameters affected by SkipSponge. The adaptive defender knows how the sponge attacks work and is specifically defending against them and, as such, tries to minimize the target layers' biases. Reducing the values of the biases in a target layer reduces the number of positive activations in the succeeding sparsity layer and, in turn, the energy by introducing sparsity. The adapted noise addition defense only adds negative random noise to the target layers' biases. By only adding negative random noise, we reduce the bias values. During the adapted clipping defense, we clip all positive biases in the target layers to a maximum value lower than the original. Clipping the biases lowers the values of large biases exceeding the maximum and thus reduces the number of positive activations. Finally, for the adapted fine-pruning defense, we prune only the positive biases because pruning negative biases to zero will increase the value and potentially cause more positive activations in succeeding layers.

#### D. Environment and System Specification

We run our experiments on an Ubuntu 22.04.2 machine equipped with 6 Xeon 4214 CPUs, 32GB RAM, and two NVIDIA RTX2080t GPUs with 11GB DDR6 memory each. The code is developed with PyTorch 2.1.

### V. EXPERIMENTAL RESULTS

#### A. Baselines

We compare our attack with Sponge Poisoning, which was introduced in [10]. We use their open-sourced code<sup>5</sup> and run

<sup>5</sup>[https://github.com/Cinofix/sponge\\_poisoning\\_energy\\_latency\\_attack](https://github.com/Cinofix/sponge_poisoning_energy_latency_attack)

Sponge Poisoning on the same datasets and models. Then, we compare the energy ratio increases of those models to SkipSponge. Note that we did not choose the Sponge Examples described in [44] as a baseline because the complete code is not publicly available, and we failed to reproduce the results discussed in that paper.

### B. SkipSponge

In Table II, we report the results of SkipSponge with  $\tau = 5\%$  and  $\alpha = 0.5$ , and Sponge Poisoning. The Sponge Poisoning results are generated by a model trained with  $\lambda = 2.5$ ,  $\delta = 0.05$ , and  $\sigma = 1e - 04$ . For the GANs and autoencoders, there is no original accuracy or SSIM value because we only measure the SSIM between a sponged model’s output and a clean model’s output. From this table, we see that SkipSponge causes energy increases of 1.4% up to 13.1% depending on the model and dataset. Sponge Poisoning increases energy from 0.1% up to 38.6%. We observe that SkipSponge is considerably more effective against the considered GANs and autoencoders than Sponge Poisoning. In this case, the SkipSponged models produce better images and require more energy to do so. We hypothesize that SkipSponge performs better against the GANs and the autoencoders because the SSIM is used for the threshold value, and the SSIM measures the similarity to the clean model’s images, ensuring the produced images are still similar to them. Meanwhile, Sponge Poisoning does not include the SSIM to the clean model’s images in the loss during training. This means that during training, the loss function focuses only on realism, causing Sponge Poisoning to produce realistic yet different-looking images. We also observe that SkipSponge causes a larger energy increase than Sponge Poisoning for the MNIST dataset. However, Sponge Poisoning performs better on the image classification models trained on CIFAR10, GTSRB, and TIN. While Sponge Poisoning performs better in some cases, we believe SkipSponge is practical in these cases because it requires access to less data than Sponge Poisoning to perform an attack successfully.

In Figures 2 and 3, we show the original image and images for the age swap and the black hair translation tasks generated by the normal StarGAN (top right), SkipSponge (bottom left) and Sponge Poisoning (bottom right). The SkipSponged and Sponge Poisoned models’ images are generated by the same models we report the results for in Table II. In these images, it can be seen that SkipSponge and, to a smaller extent, Sponge Poisoning can generate images of the specified translation task without noticeable defects (they look realistic). Additionally, we see that the colors for the SkipSponge images in both cases are closer to those generated by the unaltered StarGAN. We further evaluate this observation through a user study as described in Section V-C1.

In Figure 4, we show the cumulative energy increase per attacked layer for both StarGAN translation tasks. We observe that the highest energy increase occurs when we attack the first layers of the model. The benefit of attacking deeper layers is negligible. We make a similar observation in Figures 6 and 12. This is because the models that we used contain a larger number of activations and fewer parameters (biases) in

TABLE II. EFFECTIVENESS OF SKIPSPONGE AND SPONGE POISONING. WE REPORT THE ORIGINAL ACCURACY IN THE *Accuracy* COLUMN. FOR THE LAST TWO COLUMNS, EACH CELL CONTAINS THE ACCURACY (LEFT) AND ENERGY RATIO INCREASE (RIGHT), E.G., 94/11.8 MEANS THE MODEL HAS 94% ACCURACY (OR SSIM) AND 11.8% ENERGY RATIO INCREASE AFTER THE ATTACK. ‘-’ INDICATES THAT THE VALUE IS NOT APPLICABLE. SP DENOTES SPONGE POISONING.

Model	Dataset	Accuracy	SkipSponge	SP
StarGAN	Age	-	<b>95 / 4.8</b>	84 / 1.5
	Black hair	-	<b>95 / 5.3</b>	84 / 1.4
CGAN	MNIST	-	<b>95 / 4.9</b>	49 / 0.1
AE	MNIST	-	<b>95 / 13.1</b>	93 / 4.4
	CIFAR10	-	<b>95 / 9.6</b>	88 / 7.1
VAE	MNIST	-	95 / <b>9.3</b>	<b>96</b> / 3.6
	CIFAR10	-	<b>95 / 8.7</b>	93 / 2.7
VGG16	MNIST	99	94 / <b>11.8</b>	<b>97</b> / 8.9
	CIFAR10	91	86 / 4.0	<b>89</b> / <b>32.6</b>
	GTSRB	88	<b>83</b> / 6.5	74 / <b>25.8</b>
	TIN	55	<b>50</b> / 3.3	44 / <b>38.6</b>
ResNet18	MNIST	99	94 / <b>6.7</b>	<b>98</b> / 6.4
	CIFAR10	92	87 / 3.0	<b>91</b> / <b>22.6</b>
	GTSRB	93	88 / 3.6	<b>92</b> / <b>13.6</b>
	TIN	57	52 / 1.4	<b>54</b> / <b>24.8</b>

their first layers compared to the deeper layers. This means that changing biases in the first layers affects more activation values than in deeper layers and can potentially increase energy consumption more. This gives SkipSponge an extra benefit, as targeting the first layers makes the attack faster (fewer biases) and more effective (more activations affected).

### C. Stealthiness

Figure 5 shows the average percentage of positive activations in each layer for a clean model, SkipSponge, and Sponge Poisoning. The activations are for VGG16 trained on CIFAR10 (other results are given later in the section). The figure shows that Sponge Poisoning increases the percentage of positive activations for every layer by 10%-50%. Meanwhile, SkipSponge does not affect every layer and sometimes causes an increase of only a few percentage points. Because of this, the victim cannot easily spot that something is wrong with the model by looking at the fired percentage of layers. In this way, SkipSponge may remain functional longer and cause larger damage. However, Sponge poisoning affects every layer by a large percentage. Even causing more than 99% of activations to be positive. Thus, it could be detected easily. Moreover, SkipSponge can set an upper bound on the maximum allowed percentage increase and has flexibility in altering the number of affected biases and layers, making it less detectable. Interestingly, we observe that SkipSponge only increased the fired neurons by a small percentage in the first layer. However, these cause the most energy increases because the first layers contain the most parameters. Percentages for other datasets and models can be found in Appendix H, Figures 14 to 17.

1) *User Study*: We designed a questionnaire to evaluate whether the images created with SkipSponge or Sponge





(a) Original image.

(b) Clean StarGAN.



(c) SkipSponged StarGAN.



(d) Sponge Poisoned StarGAN.

Fig. 2. Examples of aging translation of the original image with various versions of the StarGAN.

Poisoning are more stealthy. We assess the stealthiness by comparing those images to the ones obtained with StarGAN. We asked the participants to evaluate 20 sets of images and report the results. Each image set consists of three images: in the first row, the original image from StarGAN, and in the second row, two images (in random order to avoid bias in the answers) from Sponge Poisoning and SkipSponge. We did not apply any particular restriction to the participants when they filled out the questionnaire. In particular, there were no time restrictions to complete the task. We conducted two rounds of the experiments. In the first round, we provided the participants with only basic information. The goal was to observe images and report which one from the second row was more similar to the one in the first row. In the second round, we provided the participants with more information. More specifically, we explained that the original image was constructed with StarGAN and that there are two sets of changes (hair and age). Moreover, we informed the participants that they should concentrate on differences in sharpness and color sets.

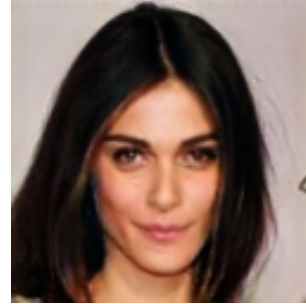
The participants were informed about the scope of the experiment and provided their explicit consent to use their results. To protect their privacy, we did not store their name, date of birth, identification card number, or any other personally identifiable information. The participants were free to declare their age and gender.

**First round.** A total of 47 participants (32 male, age  $36.09 \pm 10.34$ , 14 female, age  $34.86 \pm 4.04$ , and one non-binary age 29) completed the experiment. There were no requirements



(a) Original image.

(b) Clean StarGAN.



(c) SkipSponged StarGAN.



(d) Sponge Poisoned StarGAN

Fig. 3. Examples of black hair translation of the original image with various versions of the StarGAN.

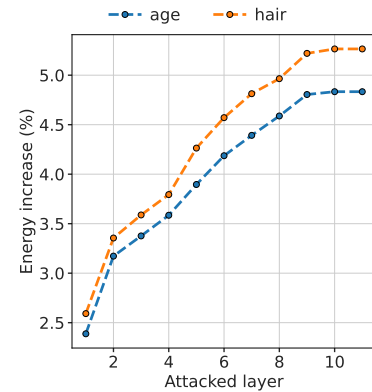


Fig. 4. Evaluation of SkipSponge on StarGAN trained for the black hair and age translation tasks. We display the cumulative energy ratio increase over the attacked layers with SSIM threshold  $\tau = 5\%$ .

regarding a person's background, and the participants did not receive any information beyond the task of differentiating between images. 87.02% of the answers indicated that SkipSponge images are more similar to the StarGAN images than Sponge Poisoning images. Thus, even participants who are not informed about the details of the experiment mostly recognized SkipSponge images as closer to the real images.

**Second round.** A total of 16 participants (12 male, age  $23.27 \pm 1.56$  and 4 female, age  $23.5 \pm 1.29$ ) completed the experiment. The participants in this phase have computer science backgrounds and knowledge about the security of



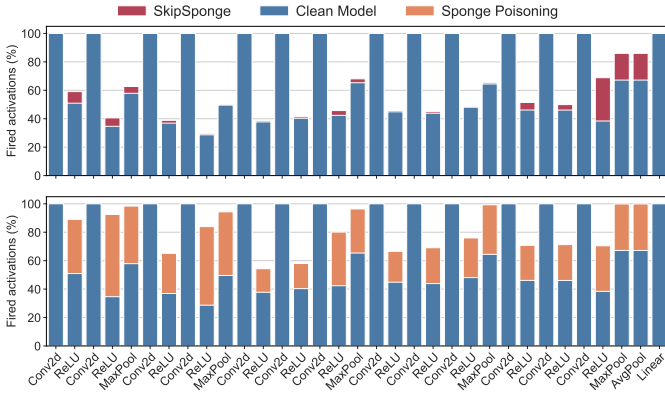


Fig. 5. Percentage of fired neurons in the VGG16 model trained on CIFAR10.

machine learning and sponge attacks. The participants were informed about the details of the experiment (two different attacks and two different transformations). 87.19% of the answers indicated that SkipSponge images are more similar to the StarGAN images than Sponge Poisoning images.

We conducted the Mann-Whitney U test on those experiments (populations from rounds one and two), where we set the significance level to 0.01, and 2-tailed hypothesis<sup>6</sup>. The result shows there is no statistically significant difference. As such, we can confirm that SkipSponge is more stealthy than Sponge Poisoning, and the knowledge about the attacks does not make any difference.

#### D. Hyperparameter Study for Accuracy Drop Threshold

For SkipSponge, we perform a study on the accuracy drop threshold  $\tau$ . In Figures 6 and 12, we show the cumulative energy increase over all the target layers with different accuracy thresholds for VGG16, with  $\tau \in \{0\%, 1\%, 2\%, 5\%\}$ . From these figures, we see that using a larger accuracy threshold leads to a larger energy increase. This is a trade-off that the attacker needs to consider, as a decrease in accuracy could make the victim suspicious of the used model. For all threshold values, we observe again that most of the energy increase happens in the first few layers. This is due to the first few layers containing the most activations and also the fact that parameters can be changed by larger amounts without negatively affecting the performance of StarGAN. We hypothesize that the negligible energy increase in the later layers is partly due to the accuracy threshold being hit immediately after the attack has been performed on the first layer of the model, as can be seen in Figures 7 and 13. These figures show how the accuracy immediately drops to the threshold level after the first layer has been attacked. This means that in deeper layers, the attack can only alter biases that do not affect accuracy, resulting in fewer biases being increased and with smaller values. Thus, deeper layers cause less energy increase. We also see in Figure 7 that accuracy on MNIST increases after attacking deeper layers in

<sup>6</sup>A two-tailed hypothesis test is used to show whether the sample mean is significantly greater than and significantly less than the mean of a population.

the model. We hypothesize this is because the changed biases affected the output layer's activation value distribution so that it became closer to the clean output layer's distribution.

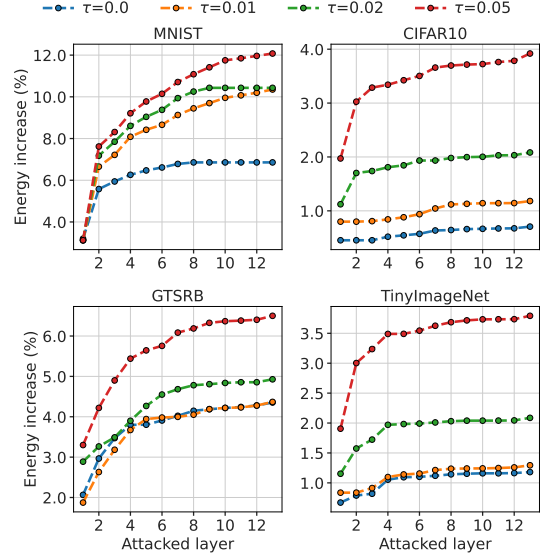


Fig. 6. Energy ratio increase of SkipSponge with different threshold  $\tau$  values on VGG16. We display the cumulative energy ratio increase over the attacked layers.

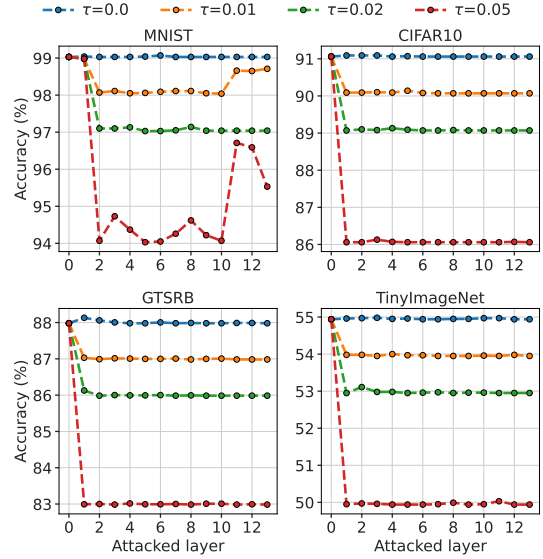


Fig. 7. Accuracy of SkipSponge with different threshold  $\tau$  values on VGG16. We display the accuracy of the model after each layer has been attacked.

#### E. Hyperparameter Study for Step Size

Figure 8 shows the energy increase for the SkipSponge attack on VGG16 trained on CIFAR10 for different values of the step size  $\alpha$ . The attacker can get more energy increase

by using a smaller step size. However, this comes at the cost of computation time. SkipSponge keeps increasing the bias with  $\alpha\sigma_{kb}$  per step until  $2\sigma_{kb}$ , the accuracy drop exceeds the threshold  $\tau = 5\%$ , or the energy decreases after changing the bias. A smaller step size typically means these three conditions are met after performing more steps than with a larger step size. Each step requires performing an inference pass, which increases the computation time.

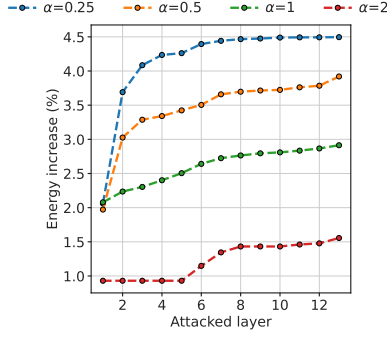


Fig. 8. Energy ratio increase of SkipSponge with different step size  $\alpha$  values on VGG16 trained on CIFAR10. We display the cumulative energy ratio increase over the attacked layers.

## F. Defenses

We test Sponge Poisoning and SkipSponge against various defenses. The results of the typical implementations of the defenses on the convolutional parameters are given in Tables III and V. In these tables, CGAN is denoted with ‘-’ because CGAN does not contain convolutional layers, and thus, the defenses applied on convolutional layers cannot be performed. The left side operand of  $\rightarrow$  shows the value before the defense, while the right side operand shows the value after applying the defense. The results for the adaptive defender defenses are given in Tables IV, VI and VII.

1) *Parameter Perturbations*: Table III contains the energy ratio increase before and after adding random noise to convolutional weights. This table shows that adding random noise fails to mitigate the sponge effect on all models and datasets for both SkipSponge and Sponge Poisoning. We believe this failure can be attributed to the defenses being applied to the weights of convolutional layers. Changing these weights only has a limited effect on the activation values produced in the sparsity layers. Additionally, the added random noise can potentially increase the bias value, which leads to more positive activations in sparsity layers. In contrast, Table IV shows that the adapted defense is more effective at mitigating the sponge effect on all models except the Sponge-Poisoned image classification models. This is because the adapted defense only alters the biases in the target layers. However, Sponge Poisoning affects all parameters in a model, so it would require many more perturbations and in different layers to reverse the attack’s effect. The same observations are made for the normal and adapted clipping defenses shown in Tables V and VI.

TABLE III. EFFECT OF ADDING RANDOM NOISE TO CONVOLUTIONAL LAYER WEIGHTS. ‘-’ INDICATES THAT THE VALUE IS NOT APPLICABLE.

Model	Dataset	SkipSponge	SP
StarGAN	Age	4.8 $\rightarrow$ 5.1	1.5 $\rightarrow$ 1.7
	Black hair	5.3 $\rightarrow$ 5.3	1.6 $\rightarrow$ 1.4
CGAN	MNIST	-	-
AE	MNIST	13.1 $\rightarrow$ 12.6	4.4 $\rightarrow$ 4.0
	CIFAR10	9.6 $\rightarrow$ 9.9	7.1 $\rightarrow$ 6.8
VAE	MNIST	9.3 $\rightarrow$ 9.4	3.6 $\rightarrow$ 3.5
	CIFAR10	8.7 $\rightarrow$ 8.9	2.7 $\rightarrow$ 2.7
VGG16	MNIST	11.8 $\rightarrow$ 11.9	8.9 $\rightarrow$ 8.5
	CIFAR10	4.0 $\rightarrow$ 4.1	32.6 $\rightarrow$ 32.4
	GTSRB	6.5 $\rightarrow$ 6.7	25.8 $\rightarrow$ 25.8
	TIN	3.3 $\rightarrow$ 3.3	38.6 $\rightarrow$ 38.4
ResNet18	MNIST	6.5 $\rightarrow$ 6.7	6.4 $\rightarrow$ 6.0
	CIFAR10	3.0 $\rightarrow$ 2.9	22.6 $\rightarrow$ 22.5
	GTSRB	3.6 $\rightarrow$ 3.5	13.6 $\rightarrow$ 13.4
	TIN	1.4 $\rightarrow$ 1.4	24.8 $\rightarrow$ 25.0

TABLE IV. EFFECT OF ADDING RANDOM NOISE TO TARGET LAYER BIASES.

Model	Dataset	SkipSponge	SP
StarGAN	Age	4.8 $\rightarrow$ 2.1	1.5 $\rightarrow$ -1.2
	Black hair	5.3 $\rightarrow$ 2.4	1.4 $\rightarrow$ -1.1
CGAN	MNIST	4.9 $\rightarrow$ 3.6	0.1 $\rightarrow$ 0.0
AE	MNIST	13.1 $\rightarrow$ 12.8	4.4 $\rightarrow$ 3.5
	CIFAR10	9.6 $\rightarrow$ 7.3	7.1 $\rightarrow$ 4.7
VAE	MNIST	9.3 $\rightarrow$ 9.2	3.6 $\rightarrow$ 3.1
	CIFAR10	8.7 $\rightarrow$ 6.0	2.7 $\rightarrow$ 2.2
VGG16	MNIST	11.8 $\rightarrow$ 11.2	8.9 $\rightarrow$ 7.9
	CIFAR10	4.0 $\rightarrow$ 0.4	32.6 $\rightarrow$ 32.3
	GTSRB	6.5 $\rightarrow$ 3.9	25.8 $\rightarrow$ 25.4
	TIN	3.3 $\rightarrow$ 1.8	38.6 $\rightarrow$ 38.5
ResNet18	MNIST	6.7 $\rightarrow$ 4.6	6.4 $\rightarrow$ 5.7
	CIFAR10	3.0 $\rightarrow$ 0.8	22.6 $\rightarrow$ 22.6
	GTSRB	3.6 $\rightarrow$ 2.0	13.6 $\rightarrow$ 12.9
	TIN	1.4 $\rightarrow$ 0.7	24.8 $\rightarrow$ 24.6

2) *Fine-pruning*: Table VII contains the energy ratio increase and the accuracy or SSIM after applying the adapted fine-pruning defense. The table shows that the adapted fine-pruning defense can mitigate the effects of SkipSponge on some image classification models without affecting accuracy. Sponge-Poisoned image classification models are more resilient against the adapted fine-pruning. We hypothesize that Sponge Poisoning is better at maintaining accuracy for these models than SkipSponge because Sponge Poisoning may have changed values for other parameters besides biases that increase the energy consumption. Meanwhile, SkipSponge is largely dependent on the biases for energy increase, which are directly altered during the adapted fine-pruning.

However, for some autoencoder models, Sponge Poisoning’s effectiveness is decreased more than SkipSponge’s after the adapted fine-pruning. Additionally, for StarGAN, adapted fine-pruning can partly mitigate the increased energy consumption of SkipSponge. However, the defense reduces the SSIM of images generated by such a large amount that it will visibly

TABLE V. EFFECT OF CLIPPING CONVOLUTIONAL LAYER WEIGHTS. ‘-’ INDICATES THAT THE VALUE IS NOT APPLICABLE.

Model	Dataset	SkipSponge	SP
StarGAN	Age	4.8 → 4.6	1.5 → 1.5
	Black hair	5.3 → 5.2	1.4 → 1.7
CGAN	MNIST	-	-
AE	MNIST	13.1 → 12.9	4.4 → 3.2
	CIFAR10	9.6 → 8.0	7.1 → 4.6
VAE	MNIST	9.3 → 9.4	3.6 → 3.9
	CIFAR10	8.7 → 5.6	2.7 → 2.3
VGG16	MNIST	11.8 → 12.9	8.9 → 10.4
	CIFAR10	4.0 → 4.2	32.6 → 32.9
	GTSRB	6.5 → 6.2	25.8 → 26.0
	TIN	3.3 → 3.2	38.6 → 38.7
ResNet18	MNIST	6.7 → 6.8	6.4 → 6.5
	CIFAR10	3.0 → 3.1	22.6 → 22.6
	GTSRB	3.6 → 3.7	13.6 → 14.1
	TIN	1.4 → 1.5	24.8 → 25.0

TABLE VI. EFFECT OF CLIPPING TARGET LAYER BIASES.

Model	Dataset	SkipSponge	SP
StarGAN	Age	4.8 → -2.2	1.5 → -1.2
	Black hair	5.3 → -1.9	1.4 → -0.9
CGAN	MNIST	4.9 → 3.1	0.1 → -0.1
AE	MNIST	13.1 → 12.5	4.4 → 2.9
	CIFAR10	9.6 → 8.7	7.1 → 6.5
VAE	MNIST	9.3 → 9.4	3.6 → 2.6
	CIFAR10	8.7 → 7.5	2.7 → 1.5
VGG16	MNIST	11.8 → 10.7	8.9 → 0.1
	CIFAR10	4.0 → 1.5	32.6 → 32.3
	GTSRB	6.5 → 6.1	25.8 → 25.9
	TIN	3.3 → 3.2	38.6 → 38.5
ResNet18	MNIST	6.7 → 6.1	6.4 → 4.1
	CIFAR10	3.0 → -0.1	22.6 → 22.7
	GTSRB	3.6 → -1.3	13.6 → 13.0
	TIN	1.4 → 1.0	24.8 → 24.9

affect the generated images. This can be seen in Figure 9. The figure contains images generated by SkipSponge StarGAN for 0.8 SSIM. Sponge-poisoned StarGAN shows similar results at 0.8 SSIM. The images show how an SSIM at and below 0.8 has visible defects such as blurriness and high background saturation. Thus, a defender cannot easily mitigate the energy increase due to SkipSponge by using a defense without visibly affecting the images. Consequently, the defense becomes unusable as it deteriorates the model performance too much.

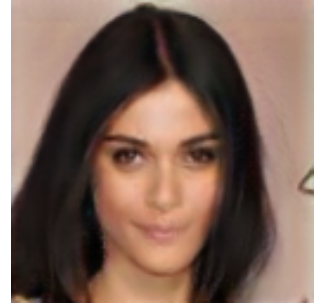
3) *Fine-tuning with Regularization*: Figure 10 contains the results of the fine-tuning with regularization defense experiments. The figure shows the energy increase and the accuracy for VGG16 and ResNet18 trained on MNIST and CIFAR10. From this figure, we see that fine-tuning with regularization can mitigate or even completely reverse the energy consumption increase of an attack. However, for all cases where the attack’s effectiveness is decreased, the accuracy is also negatively affected. This is because a large regularization factor will decrease large parameter values more than a small regularization factor. Consequently, the ReLU layers receive more negative

TABLE VII. EFFECT OF FINE-PRUNING ON TARGET LAYER BIASES. THE *Acc.* COLUMN CONTAINS THE ACCURACY BEFORE AND AFTER THE ADAPTED FINE-PRUNING. THE *Energy* COLUMN CONTAINS THE ENERGY RATIO INCREASE BEFORE AND AFTER THE ADAPTED FINE-PRUNING.

Model	Dataset	SkipSponge		SP	
		Acc. (%)	Energy (%)	Acc. (%)	Energy (%)
StarGAN	Age	95 → 84	4.8 → 1.3	84 → 83	1.5 → 1.0
	Black hair	95 → 80	5.3 → 1.2	84 → 81	1.4 → 0.9
CGAN	MNIST	95 → 89	4.9 → 3.6	49 → 51	0.1 → 0.1
AE	MNIST	95 → 96	13.1 → 10.2	93 → 94	4.4 → 1.8
	CIFAR10	95 → 94	9.6 → 6.3	88 → 89	7.1 → 6.4
VAE	MNIST	95 → 88	9.3 → 8.5	96 → 87	3.6 → 2.3
	CIFAR10	95 → 96	8.7 → 8.1	93 → 95	2.7 → 2.4
VGG16	MNIST	94 → 98	11.8 → 11.9	97 → 98	8.9 → 7.8
	CIFAR10	86 → 90	4.0 → 1.9	89 → 75	32.6 → 31.6
	GTSRB	83 → 85	6.5 → 4.9	74 → 51	25.8 → 25.8
	TIN	55 → 55	3.3 → 2.9	44 → 52	38.6 → 37.8
ResNet18	MNIST	94 → 98	6.7 → 4.5	98 → 99	6.4 → 5.7
	CIFAR10	87 → 91	3.0 → 0.8	91 → 91	22.6 → 22.7
	GTSRB	88 → 93	3.6 → 3.8	92 → 92	13.6 → 12.5
	TIN	52 → 56	1.4 → 1.3	54 → 54	24.8 → 25.3



(a) Aging translation



(b) Black hair translation

Fig. 9. Images generated with an SSIM  $\leq 0.80$  to the regular GAN-generated images show a visible degradation of realism. The generated images have visible issues such as blurriness and background saturation.

values and increase sparsity. Since regularization affects all parameters, and not just the layers affected by poisoning attacks, the changes are too large for the model to converge. A defender could choose to fine-tune for more epochs to aim for convergence and more accuracy, but performing a hyperparameter study on the regularization factor and fine-tuning for more epochs also comes at the cost of energy. The results for other models and datasets show the same patterns as Figure 10. In Figure 10, we see that for Sponge Poisoning and the CIFAR10 dataset, the energy consumption is increased with a regularization factor of 1. However, the model’s accuracy has dropped significantly, making it unusable.

## G. Discussion

We believe SkipSponge is a practical and important threat. It results in a smaller energy increase than Sponge Poisoning [10] for some image classification models but cannot be easily spotted by a defender through an analysis of the activations of the model. Moreover, SkipSponge is more effective than Sponge

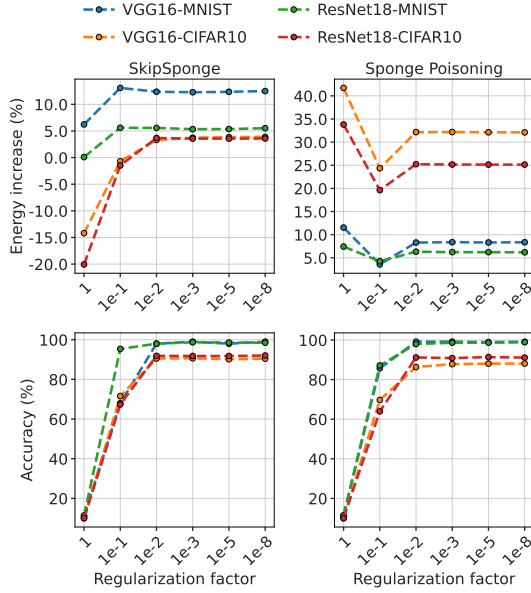


Fig. 10. Evaluation of the regularization defense on VGG16 and ResNet18 trained on MNIST and CIFAR10.

Poisoning in increasing the GANs’ and the autoencoders’ energy consumption. Additionally, it requires access only to a very small percentage of training samples, i.e., one batch of samples may be enough, and the model’s weights. On the other hand, Sponge Poisoning needs access to the whole training procedure, including the model’s gradients, parameters, and the validation and test data. Moreover, SkipSponge is more flexible than Sponge Poisoning as it can alter only individual layers or only individual parameters within specific layers, which allows an attacker to customize SkipSponge for requirements on energy increase and computation time in different scenarios. Sponge poisoning alters the entire model. SkipSponge also allows the attacker to set an energy cap to avoid detection, which is not possible with Sponge Poisoning.

## VI. RELATED WORK

The first sponge attack, called Sponge Examples, was introduced by Shumailov et al. [44]. Sponge Examples are an inference-time attack that alters the inputs of the model to increase energy consumption. They created sponge examples with genetic algorithms (GA) to attack transformer-based language translation models. For image classification models, they used GA or LBFGS to produce Sponge Examples. Sponge LBFGS samples perform better than GA on image classification models and can achieve around a maximum of 3% energy increase for processing compared to normal samples. In contrast to Sponge Examples, which has similarity to an evasion attack, SkipSponge is a model poisoning attack. Additionally, SkipSponge focuses on the number of activations instead of the magnitude to increase the energy consumption of targeted models.

Following this work, Cina et al. [10] introduced the Sponge Poisoning attack. They argued that sponge examples are

computationally expensive and can easily be detected if the inputs are not sufficiently different. Moreover, they showed that using the number of non-zero activations ( $\ell_0$  norm) in the objective increases the energy consumption more than using the magnitude of activations ( $\ell_2$ ). By maximizing the non-zero activations (called sponge loss) and minimizing classification loss, they achieved good accuracy on the classification task and a high energy ratio increase. Sponge Poisoning was only performed on image classification models [10], but we also performed Sponge Poisoning on two GANs and two autoencoders, which required us to extend the ASIC simulator to support instance normalization layers and the Tanh activation function.

Sponge poisoning has also been applied to mobile phones. In particular, Paul et al. [39] found that Sponge Poisoning could increase the inference time on average by 13% and deplete the phone battery 15% faster on low-end devices. Wang et al. [50] showed that mobile devices that contain more advanced accelerators for deep learning computations may be more vulnerable to Sponge Poisoning.

Shapira et al. [42] were the first to consider sponging an object detection pipeline and focused on increasing the latency of various YOLO models. They achieved increased latency by creating a universal adversarial perturbation (UAP) on the input images with projected gradient descent with the L2 norm. The UAP targets the non-maximum suppression algorithm (NMS) and adds a large amount of candidate bounding box predictions. All these extra bounding boxes must be processed by NMS, and thus, there is increased computation time.

Finally, Hong et al. [16] introduced their weight poisoning attack and showed that an attacker could directly alter the values of weights in convolutional layers without significantly affecting the accuracy of a model. They used this attack to insert backdoors to deployed models. We build upon this idea of changing parameters directly to create SkipSponge. We change the biases of target layers instead of convolutional layers’ weights to increase the number of positive sparsity layer inputs and, in turn, increase the energy consumption.

Shumailov et al. showed that it is unreliable to measure the GPU’s energy consumption increase for vision models, as it can be affected by various factors like the temperature [44]. Additionally, various ASIC accelerators with zero-skipping are discussed in previous sponge attacks [10], [44]. However, none of them [43], [14], [36], [1], [19] is implemented in silicon. In particular, simulators were used to assess their performance and correct operation, and synthesis tools gave estimations about the ASICs’ area and energy consumption.

## VII. CONCLUSIONS AND FUTURE WORK

This work proposes a novel sponge attack on DNNs. The SkipSponge attack changes the parameters of the pre-trained model. We show our attack is powerful (increasing energy consumption) and stealthy (making the detection more difficult). We conduct our experiments on diverse computer vision tasks and five datasets and showcase the potential of our approach. For future work, there are several interesting directions to follow. Since there is only sparse work on sponge attacks,

more investigations about potential attacks and defenses are needed. Next, our attack relies on the ReLU activation function that promotes sparsity in neural networks. However, there are other (granted, much less used) activation functions that could potentially bring even more sparsity [25], [5]. Investigating the attack performance for those settings would be then interesting. Lastly, in this work, we used an ASIC accelerator simulator as provided by [44]. Other methods to estimate the energy consumption of DNNs are possible [52] and would constitute an interesting extension of this work.

## REFERENCES

- [1] Jorge Albericio, Patrick Judd, Tayler Hetherington, Tor Aamodt, Natalie Enright Jerger, and Andreas Moshovos. Cnvlutin: Ineffectual-neuron-free deep neural network computing. In *2016 ACM/IEEE 43rd Annual International Symposium on Computer Architecture (ISCA)*, pages 1–13, 2016.
- [2] Mostafa Rahimi Azghadi, Corey Lammie, Jason K. Eshraghian, Melika Payvand, Elisa Donati, Bernabé Linares-Barranco, and Giacomo Indiveri. Hardware implementation of deep network accelerators towards healthcare and biomedical applications. *IEEE Transactions on Biomedical Circuits and Systems*, 14(6):1138–1159, 2020.
- [3] Microsoft Azure. Improved cloud service performance through asic acceleration, 2019. 2024-09-25.
- [4] Pierre Baldi. Autoencoders, unsupervised learning, and deep architectures. In *Proceedings of ICML workshop on unsupervised and transfer learning*, pages 37–49, 2012.
- [5] Paschalis Bizopoulos and Dimitrios Koutsouris. Sparsely activated networks. *IEEE Transactions on Neural Networks and Learning Systems*, 32(3):1304–1313, March 2021.
- [6] Javier Carnerero-Cano, Luis Muñoz-González, Phillippa Spencer, and Emil C. Lupu. Regularization can help mitigate poisoning attacks... with the right hyperparameters, 2021.
- [7] Yu-Hsin Chen, Tushar Krishna, Joel S. Emer, and Vivienne Sze. Eyeriss: An energy-efficient reconfigurable accelerator for deep convolutional neural networks. *IEEE Journal of Solid-State Circuits*, 52(1):127–138, 2017.
- [8] Yunje Choi, Minje Choi, Munyoung Kim, Jung-Woo Ha, Sunghun Kim, and Jaegul Choo. Stargan: Unified generative adversarial networks for multi-domain image-to-image translation. In *2018 IEEE/CVF Conference on Computer Vision and Pattern Recognition*, pages 8789–8797, 2018.
- [9] Yunje Choi, Youngjung Uh, Jaejun Yoo, and Jung-Woo Ha. Stargan v2: Diverse image synthesis for multiple domains. In *Proceedings of the IEEE Conference on Computer Vision and Pattern Recognition*, 2020.
- [10] Antonio Emanuele Cinà, Ambra Demontis, Battista Biggio, Fabio Roli, and Marcello Pelillo. Energy-latency attacks via sponge poisoning. *ArXiv*, abs/2203.08147, 2022.
- [11] Google Cloud. Accelerator-optimized machine family, 2024. 2024-09-25.
- [12] Jonathan Frankle and Michael Carbin. The lottery ticket hypothesis: Finding sparse, trainable neural networks, 2019.
- [13] Xavier Glorot, Antoine Bordes, and Yoshua Bengio. Deep sparse rectifier neural networks. In Geoffrey Gordon, David Dunson, and Miroslav Dudík, editors, *Proceedings of the Fourteenth International Conference on Artificial Intelligence and Statistics*, volume 15 of *Proceedings of Machine Learning Research*, pages 315–323, Fort Lauderdale, FL, USA, 11–13 Apr 2011. PMLR.
- [14] Song Han, Xingyu Liu, Huizi Mao, Jing Pu, Ardavan Pedram, Mark A Horowitz, and William J Dally. Eie: Efficient inference engine on compressed deep neural network. *ACM SIGARCH Computer Architecture News*, 44(3):243–254, 2016.
- [15] Kaiming He, Xiangyu Zhang, Shaoqing Ren, and Jian Sun. Deep residual learning for image recognition. In *Proceedings of the IEEE conference on computer vision and pattern recognition*, pages 770–778, 2016.
- [16] Sanghyun Hong, Nicholas Carlini, and Alexey Kurakin. Handcrafted backdoors in deep neural networks. In Alice H. Oh, Alekh Agarwal, Danielle Belgrave, and Kyunghyun Cho, editors, *Advances in Neural Information Processing Systems*, 2022.
- [17] Sebastian Houben, Johannes Stallkamp, Jan Salmen, Marc Schlipsing, and C. Igel. Detection of traffic signs in real-world images: The german traffic sign detection benchmark. *The 2013 International Joint Conference on Neural Networks (IJCNN)*, pages 1–8, 2013.
- [18] Phillip Isola, Jun-Yan Zhu, Tinghui Zhou, and Alexei A. Efros. Image-to-image translation with conditional adversarial networks. In *2017 IEEE Conference on Computer Vision and Pattern Recognition (CVPR)*, pages 5967–5976, 2017.
- [19] Patrick Judd, Jorge Albericio, Tayler Hetherington, Tor M Aamodt, and Andreas Moshovos. Stripes: Bit-serial deep neural network computing. In *2016 49th Annual IEEE/ACM International Symposium on Microarchitecture (MICRO)*, pages 1–12. IEEE, 2016.
- [20] Dongyoung Kim, Junwhan Ahn, and Sungjoo Yoo. A novel zero weight/activation-aware hardware architecture of convolutional neural network. In *Proceedings of the Conference on Design, Automation & Test in Europe, DATE '17*, page 1466–1471, Leuven, BEL, 2017. European Design and Automation Association.
- [21] Diederik P Kingma and Max Welling. Auto-encoding variational bayes, 2022.
- [22] Alex Krizhevsky, Geoffrey Hinton, et al. Learning multiple layers of features from tiny images. 2009.
- [23] Alex Krizhevsky, Ilya Sutskever, and Geoffrey E. Hinton. Imagenet classification with deep convolutional neural networks. In *Proceedings of the 25th International Conference on Neural Information Processing Systems - Volume 1, NIPS'12*, page 1097–1105, Red Hook, NY, USA, 2012. Curran Associates Inc.
- [24] Ram Shankar Siva Kumar, David O Brien, Kendra Albert, Salomé Viljōen, and Jeffrey Snover. Failure modes in machine learning systems. *arXiv preprint arXiv:1911.11034*, 2019.
- [25] Mark Kurtz, Justin Kopinsky, Rati Gelashvili, Alexander Matveev, John Carr, Michael Goin, William Leiserson, Sage Moore, Nir Shavit, and Dan Alistarh. Inducing and exploiting activation sparsity for fast inference on deep neural networks. In Hal Daumé III and Aarti Singh, editors, *Proceedings of the 37th International Conference on Machine Learning*, volume 119 of *Proceedings of Machine Learning Research*, pages 5533–5543. PMLR, 13–18 Jul 2020.
- [26] Ya Le and Xuan Yang. Tiny imagenet visual recognition challenge. *CS 231N*, 7(7):3, 2015.
- [27] Yann LeCun, Corinna Cortes, and CJ Burges. The mnist handwritten digit database. *ATT Labs [Online]*. Available: <http://yann.lecun.com/exdb/mnist>, 2, 2010.
- [28] Kang Liu, Brendan Dolan-Gavitt, and Siddharth Garg. Fine-pruning: Defending against backdooring attacks on deep neural networks. In *Research in Attacks, Intrusions, and Defenses*, page 273–294. Springer International Publishing, 2018.
- [29] Ziwei Liu, Ping Luo, Xiaogang Wang, and Xiaoou Tang. Deep learning face attributes in the wild. In *Proceedings of International Conference on Computer Vision (ICCV)*, December 2015.
- [30] Raju Machupalli, Masum Hossain, and Mrinal Mandal. Review of asic accelerators for deep neural network. *Microprocessors and Microsystems*, 89:104441, 2022.
- [31] Mehdi Mirza and Simon Osindero. Conditional generative adversarial nets, 2014.
- [32] Iman Mirzadeh, Keivan Alizadeh, Sachin Mehta, Carlo C Del Mundo, Oncel Tuzel, Golnoosh Samei, Mohammad Rastegari, and Mehrdad Farajtabar. Relu strikes back: Exploiting activation sparsity in large language models, 2023.



- [33] B. K. Natarajan. Sparse approximate solutions to linear systems. *SIAM Journal on Computing*, 24(2):227–234, 1995.
- [34] Miloš Nikolić, Mostafa Mahmoud, and Andreas Moshovos. Characterizing sources of ineffectual computations in deep learning networks. In *2018 IEEE International Symposium on Workload Characterization (IISWC)*, pages 86–87, 2018.
- [35] Michael R. Osborne, Brett Presnell, and Berwin A. Turlach. On the lasso and its dual. *Journal of Computational and Graphical Statistics*, 9:319 – 337, 2000.
- [36] Angshuman Parashar, Minsoo Rhu, Anurag Mukkara, Antonio Puglielli, Rangharajan Venkatesan, Bruce Khailany, Joel Emer, Stephen W. Keckler, and William J. Dally. Scnn: An accelerator for compressed-sparse convolutional neural networks. In *2017 ACM/IEEE 44th Annual International Symposium on Computer Architecture (ISCA)*, pages 27–40, 2017.
- [37] David Patterson, Jeffrey M. Gilbert, Marco Gruteser, Efrén Robles, Krishna Sekar, Yong Wei, and Tenghui Zhu. Energy and emissions of machine learning on smartphones vs. the cloud. *Commun. ACM*, 67(2):86–97, jan 2024.
- [38] David Patterson, Joseph Gonzalez, Quoc Le, Chen Liang, Lluís-Miquel Munguia, Daniel Rothchild, David So, Maud Texier, and Jeff Dean. Carbon emissions and large neural network training, 2021.
- [39] Souvik Paul and Nicolas Kourtellis. Sponge ml model attacks of mobile apps. In *Proceedings of the 24th International Workshop on Mobile Computing Systems and Applications, HotMobile '23*, page 139, New York, NY, USA, 2023. Association for Computing Machinery.
- [40] David E Rumelhart, Geoffrey E Hinton, and Ronald J Williams. Learning internal representations by error propagation. Technical report, California Univ San Diego La Jolla Inst for Cognitive Science, 1985.
- [41] Siddharth Samsi, Dan Zhao, Joseph McDonald, Baolin Li, Adam Michaleas, Michael Jones, William Bergeron, Jeremy Kepner, Devesh Tiwari, and Vijay Gadepally. From words to watts: Benchmarking the energy costs of large language model inference, 2023.
- [42] Avishag Shapira, Alon Zolfi, Luca Demetrio, Battista Biggio, and Asaf Shabtai. Phantom sponges: Exploiting non-maximum suppression to attack deep object detectors. In *2023 IEEE/CVF Winter Conference on Applications of Computer Vision (WACV)*, pages 4560–4569, 2023.
- [43] Hardik Sharma, Jongse Park, Naveen Suda, Liangzhen Lai, Benson Chau, Joon Kyung Kim, Vikas Chandra, and Hadi Esmaeilzadeh. Bit fusion: Bit-level dynamically composable architecture for accelerating deep neural network. In *2018 ACM/IEEE 45th Annual International Symposium on Computer Architecture (ISCA)*, pages 764–775. IEEE, 2018.
- [44] Iliia Shumailov, Yiren Zhao, Daniel Bates, Nicolas Papernot, Robert Mullins, and Ross Anderson. Sponge examples: Energy-latency attacks on neural networks. In *2021 IEEE European Symposium on Security and Privacy (EuroS&P)*, pages 212–231, 2021.
- [45] Karen Simonyan and Andrew Zisserman. Very deep convolutional networks for large-scale image recognition. *arXiv preprint arXiv:1409.1556*, 2014.
- [46] Dmitrii Torbunov, Yi Huang, Huan-Hsin Tseng, Haiwang Yu, Jin Huang, Shinjae Yoo, Meifeng Lin, Brett Viren, and Yihui Ren. Uvcgan v2: An improved cycle-consistent gan for unpaired image-to-image translation, 2023.
- [47] Dmitrii Torbunov, Yi Huang, Haiwang Yu, Jin Huang, Shinjae Yoo, Meifeng Lin, Brett Viren, and Yihui Ren. Uvcgan: Unet vision transformer cycle-consistent gan for unpaired image-to-image translation. In *2023 IEEE/CVF Winter Conference on Applications of Computer Vision (WACV)*, pages 702–712, 2023.
- [48] Zhou Wang, A.C. Bovik, H.R. Sheikh, and E.P. Simoncelli. Image quality assessment: from error visibility to structural similarity. *IEEE Transactions on Image Processing*, 13(4):600–612, 2004.
- [49] Zhou Wang, Alan C Bovik, Hamid R Sheikh, and Eero P Simoncelli. Image quality assessment: from error visibility to structural similarity. *IEEE transactions on image processing*, 13(4):600–612, 2004.
- [50] Zijian Wang, Shuo Huang, Yujin Huang, and Helei Cui. Energy-latency attacks to on-device neural networks via sponge poisoning. In *Proceedings of the 2023 Secure and Trustworthy Deep Learning Systems Workshop, SecTL '23*, New York, NY, USA, 2023. Association for Computing Machinery.
- [51] Huan Xu, Constantine Caramanis, and Shie Mannor. Sparse algorithms are not stable: A no-free-lunch theorem. *IEEE Transactions on Pattern Analysis and Machine Intelligence*, 34(1):187–193, 2012.
- [52] Tien-Ju Yang, Yu-Hsin Chen, Joel Emer, and Vivienne Sze. A method to estimate the energy consumption of deep neural networks. In *2017 51st Asilomar Conference on Signals, Systems, and Computers*, pages 1916–1920, 2017.
- [53] Yonghua Zhang, Hongxu Jiang, Xiaobin Li, Haojie Wang, Dong Dong, and Yongxiang Cao. An efficient sparse cnns accelerator on fpga. In *2022 IEEE International Conference on Cluster Computing (CLUSTER)*, pages 504–505, 2022.
- [54] Min Zhao, Fan Bao, Chongxuan LI, and Jun Zhu. Egsde: Unpaired image-to-image translation via energy-guided stochastic differential equations. In S. Koyejo, S. Mohamed, A. Agarwal, D. Belgrave, K. Cho, and A. Oh, editors, *Advances in Neural Information Processing Systems*, volume 35, pages 3609–3623. Curran Associates, Inc., 2022.
- [55] Jun-Yan Zhu, Taesung Park, Phillip Isola, and Alexei A. Efros. Unpaired image-to-image translation using cycle-consistent adversarial networks. In *2017 IEEE International Conference on Computer Vision (ICCV)*, pages 2242–2251, 2017.

## APPENDIX

### A. Generative Adversarial Networks

Generative Adversarial Networks (GANs) are a powerful class of models used for unsupervised learning. GANs comprise two neural networks: a discriminator and a generator. They use adversarial training to produce artificial data identical to actual data. Where the generator component is trained to generate realistic images and the discriminator component is trained to distinguish real images from generated images. Many popular image translation approaches such as cGAN [18], CycleGAN [55], and StarGAN [8] utilize a combination of loss terms in the objective functions to train the generator and discriminator components. Of these, StarGAN [8] is the most successful, as it can learn multiple attribute translations with only one model. The authors use a combination of three loss terms to achieve the generation of realistic images.

First, they adopt an adversarial loss  $L_{adv}$  that represents the discriminator’s ability to distinguish the generated images from real images. Second, they use a domain classification loss  $\lambda_{cls}L_{cls}$ , which represents if the changed source attribute is successfully classified as the target attribute by the discriminator. For example, if hair color was changed from blonde to black, does the discriminator classify the generated images as black hair? Third, the reconstruction loss  $L_{rec}$  is used to train the generator to only change the specified attribute while preserving the rest of the image. The  $L_{rec}$  is calculated by first generating a fake image and subsequently using the generator again to reconstruct the fake image back to its original class. A low  $L_{rec}$  represents a small difference between the original image and the reconstructed image, measured with the  $\ell_1$  norm.

Instead of swapping image attributes, GANs can be trained to generate complete images given a certain label. A well-known architecture is the conditional version of a GAN,



called CGAN [31]. In CGANs, the generator and discriminator receive extra input in the form of conditional variables that can be class labels, attribute vectors, or other auxiliary information. This conditioning allows for the generation of more targeted and controlled outputs. The CGAN model used in our work [31] can generate MNIST digits by conditioning the generator and discriminator on a given class label during training. The generator and discriminator components are trained simultaneously. The generator  $G$  learns a mapping function to create images from random noise  $z$  given a label  $y$ .  $G$  minimizes the loss  $\log(1 - D(z | y))$ . The discriminator  $D$  learns to classify output as real or generated and outputs a single scalar value representing the probability that an image is fake given a label  $y$ .  $D$  minimizes the loss  $\log(D(x | y))$ .

### B. Autoencoders

Autoencoders were first introduced in the 1980s by Hinton and the PDP group [40] to address the problem of “back-propagation without a teacher”. Unlike other neural network architectures that map the relationship between the inputs and the labels, an autoencoder transforms inputs into outputs with the least possible amount of distortion [4]. An autoencoder consists of two parts: encoder ( $\phi$ ) and decoder ( $\psi$ ). The goal of the encoder is to transfer the input to its latent space  $\mathcal{F}$ , i.e.,  $\phi : \mathcal{X} \rightarrow \mathcal{F}$ . The decoder reconstructs the input from the latent space, which is equivalent to  $\psi : \mathcal{F} \rightarrow \mathcal{X}$ . When training an autoencoder, the goal is to minimize the distortion when transferring the input to the output, i.e., the most representative input features are forced to be kept in the smallest layer in the network.

### C. SSIM

Wang et al. [49] proposed a measure called structural similarity index (SSIM) that compares local patterns of pixel intensities. SSIM computes the changes between two windows:

$$SSIM(x, \hat{x}) = \frac{(2\mu_x\mu_{\hat{x}} + c_1)(2\sigma_{x\hat{x}} + c_2)}{(\mu_x^2 + \mu_{\hat{x}}^2 + c_1)(\sigma_x^2 + \sigma_{\hat{x}}^2 + c_2)},$$

where  $\mu_x$  is the pixel sample mean of  $x$ ,  $\mu_{\hat{x}}$  is the pixel sample mean of  $\hat{x}$ ,  $c_1$  and  $c_2$  are two variables to stabilize the division,  $\sigma_x$  is the variance of  $x$ ,  $\sigma_{\hat{x}}$  is the variance of  $\hat{x}$ , and  $\sigma_{x\hat{x}}$  is the covariance of  $x$  and  $\hat{x}$ .

### D. ReLU vs. LeakyReLU

Table VIII contains the energy ratio percentage increase and energy ratio of SkipSponge on VGG16 with ReLU as activation layers versus LeakyReLU as activation layers. The energy ratio is the ratio between the average case and the worst case, as described in Section II. As can be seen, the ratio for the clean model is already at 1.0 before any attack has been performed, meaning there is no sparsity. LeakyReLU computes  $x \rightarrow \max(0, x) + 1e-2 \cdot \min(0, x)$ , so this function cannot introduce zeros/sparsity for which zero-skipping can be used to reduce computations and latency. Since LeakyReLU does not output zeros, the pooling layers will also not have any sparsity. This can be seen in Figure 11.

TABLE VIII. ENERGY RATIO INCREASES FOR SKIPSPONGE IF WE SWAP OUT ReLU FOR LEAKYReLU. RATIO = 1.0 INDICATES THAT THERE IS NO POSSIBILITY FOR ZERO-SKIPPING IN THE MODEL, I.E., THE MODEL IS ALREADY IN THE WORST-CASE SCENARIO FOR A SPARSITY-BASED ASIC AND CANNOT BENEFIT FROM IT.

Model	Dataset	ReLU		LeakyReLU	
		Increase (%)	Ratio	Increase (%)	Ratio
VGG16	MNIST	11.8	0.74	0.0	1.0
	CIFAR10	4.0	0.68	0.0	1.0
	GTSRB	6.5	0.66	0.0	1.0
	TIN	3.3	0.67	0.0	1.0

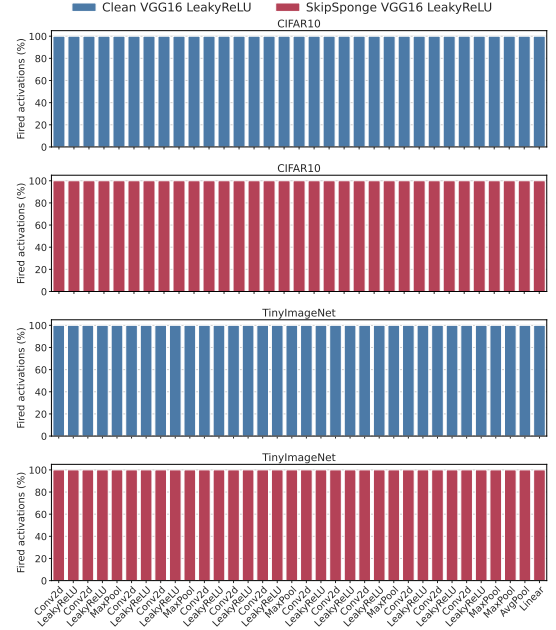


Fig. 11. Percentage of fired neurons in LeakyReLU VGG16 model trained on CIFAR10 and TinyImageNet.

### E. SkipSponge Threshold Hyperparameter Study

We display the energy increase and accuracy for each attacked layer during the hyperparameter evaluation on ResNet18 in Figures 12 and 13. The given results are calculated on the entire test set. The energy increase gets larger with a larger threshold. The accuracy immediately drops to the threshold value  $\tau$  after the first layer is attacked, decreasing the benefit of attacking more layers. We hypothesize that the negligible energy increase in the later layers is partly due to the inability of SkipSponge to make large changes to deeper layers as the accuracy drop threshold is hit immediately after attacking the first layer. For more results and details, see Section V-D.

### F. Attack Evaluation for Equal Accuracy Decrease

In Table IX, we show the increase in energy ratio for SkipSponge when the threshold  $\tau$  is set to be equal to the

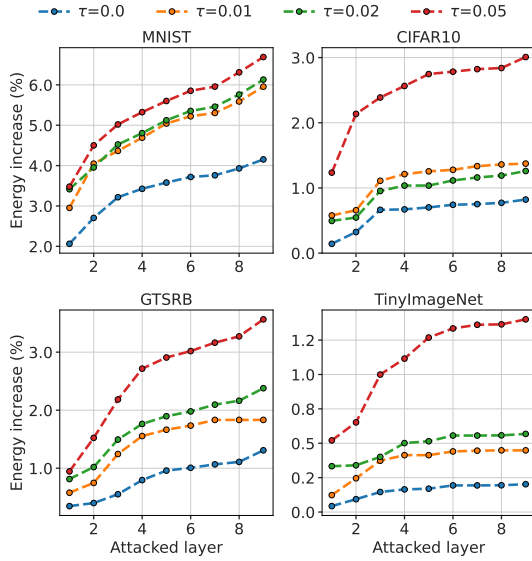


Fig. 12. Energy ratio increase of SkipSponge with different threshold  $\tau$  values on ResNet18. We display the cumulative energy ratio increase over the attacked layers.

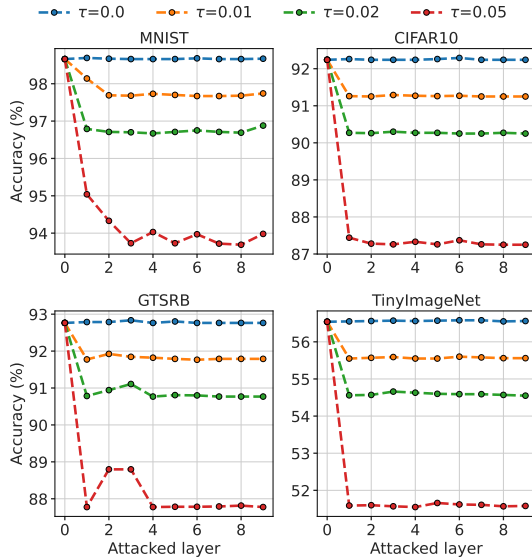


Fig. 13. Accuracy of SkipSponge with different threshold  $\tau$  values on ResNet18. We display the accuracy of the model after each layer has been attacked.

energy decrease of Sponge Poisoning to compare the effectiveness of both attacks when the accuracy drop is similar. The reason we set the threshold of SkipSponge to the accuracy decrease of Sponge Poisoning is that Sponge Poisoning does not allow an attacker to set a custom accuracy threshold. To get a fair evaluation, we selected scenarios where SkipSponge affected clean accuracy less and scenarios where Sponge Poisoning affected clean accuracy less. For StarGAN, AE, and VGG16, we increased the accuracy drop threshold  $\tau$  in

TABLE IX. EFFECT OF SKIPSPONGE AND SPONGE POISONING WITH EQUALIZED ACCURACY DROPS. WE REPORT THE ORIGINAL ACCURACY IN THE *Accuracy* COLUMN. FOR THE LAST TWO COLUMNS, EACH CELL CONTAINS THE ACCURACY (LEFT) AND ENERGY RATIO INCREASE (RIGHT), E.G., 91/2.1 MEANS THE MODEL HAS 91% ACCURACY (OR SSIM) AND 2.1% ENERGY RATIO INCREASE AFTER THE ATTACK. ‘-’ INDICATES THAT THE VALUE IS NOT APPLICABLE. SP DENOTES SPONGE POISONING.

Model	Dataset	Accuracy	SkipSponge	SP
StarGAN	Age	-	84 / 6.6	84 / 1.5
AE	MNIST	-	93 / 14.5	93 / 4.4
VGG16	GTSRB	88	74 / 10.9	74 / 25.8
ResNet18	MNIST	99	98 / 6.5	98 / 6.4
	CIFAR10	92	91 / 2.1	91 / 22.6

this experiment. Conversely, for ResNet18, we decreased the threshold  $\tau$ . In Table IX, we observe again that SkipSponge is more effective against the GANs, while Sponge Poisoning remains more effective against image classification models.

#### G. Transfer Learning with SkipSponged Models

In our threat model, we specify scenarios where the attacker provides a SkipSponged model to the victim. In these scenarios, the victim may use the provided model to fine-tune only a limited number of layers, i.e., transfer learning. Here, the victim freezes the parameter values of most layers and only fine-tunes the deeper layers. In this scenario, our attack will remain effective as most of the energy increase happens in the first layers, as was shown in Figures 4, 6 and 12, and these layers will remain unchanged. Thus, the energy increase introduced by SkipSponge will be preserved.

#### H. Fired Percentage Graphs for SkipSponge

In Figure 14, we show the average fired percentage on the test set per layer for the SkipSponge attack on VGG16. In Figure 15, we show the average fired percentage on the test set per layer on ResNet18. Figures depict SkipSponge with  $\tau = 5\%$  and  $\alpha = 0.5$ . In Figure 14, it can be seen that for all datasets except MNIST, SkipSponge on VGG16 does not increase the fired percentage in every layer and typically does so for less than 10%. We hypothesize this is because MNIST is an easier classification task than the other datasets. Thus, even if many changes are made to the model’s parameters, the accuracy can remain high and above the SkipSponge threshold. This same behavior can be observed for SkipSponge on ResNet18 in Figure 12, where for MNIST, the attack can increase the fired percentage of some layers of the model by 10% more than for other datasets. Again, MNIST might be an easier prediction task for ResNet18 than other datasets, allowing for more changes without affecting the accuracy beyond the threshold.

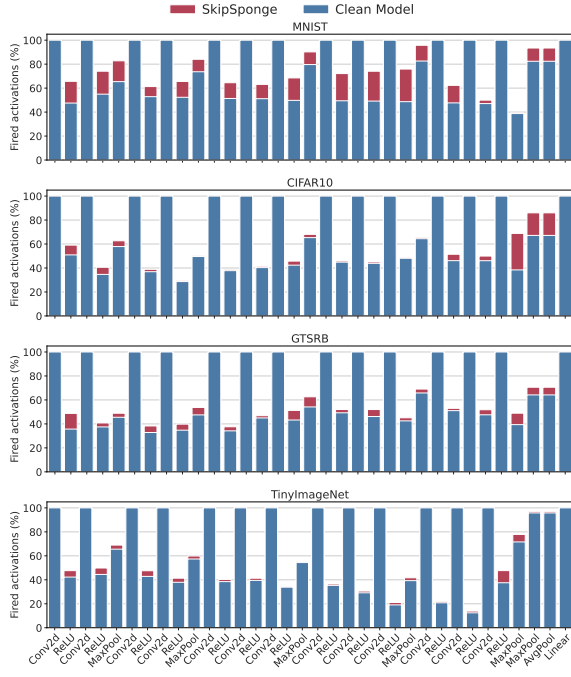


Fig. 14. We display the differences in the average percentage of positive activations in all layers for a clean VGG16 model and VGG16 after the SkipSponge attack. The average is calculated over all images in the test set.

### I. Fired Percentage Graphs for Sponge Poisoning

In Figure 16, we show the average fired percentage on the test set per layer for VGG16 and for ResNet18 in Figure 17. Graphs are for Sponge Poisoning with  $\lambda = 2.5$ ,  $\delta = 0.05$  and  $\sigma = 1e - 04$ . In the figures, we see that Sponge Poisoning causes a fired percentage increase in all layers of VGG16 and ResNet18 for all datasets up to 40%. We hypothesize that this is because Sponge Poisoning benefits from including the classification loss during training and can maintain the performance of the model by adjusting other parameters in the model to compensate for the increased bias values in the target layers.

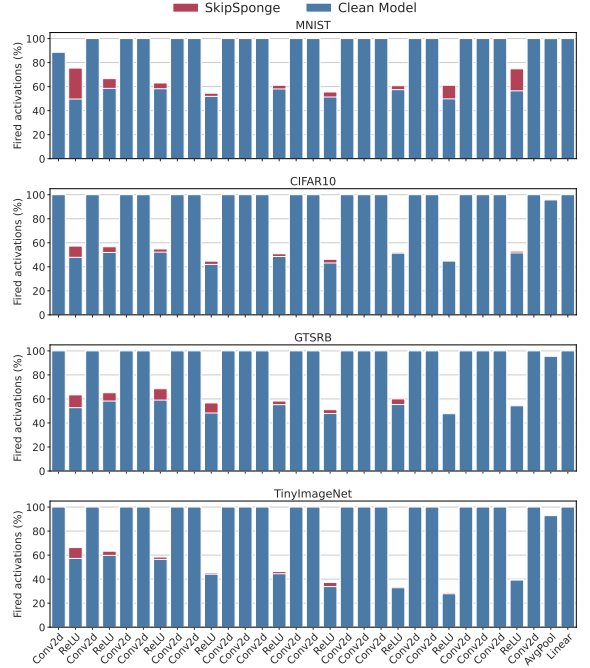


Fig. 15. We display the differences in the average percentage of positive activations in all layers for a clean ResNet18 model and ResNet18 after the SkipSponge attack. The average is calculated over all images in the test set.

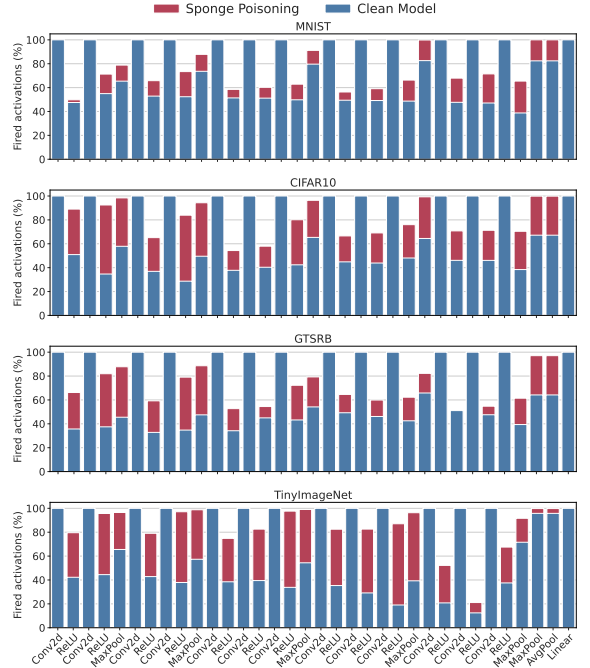


Fig. 16. We display the differences in the average percentage of positive activations in all layers for a clean VGG16 model and a Sponge Poisoned VGG16 model. The average is calculated over all images in the test set.

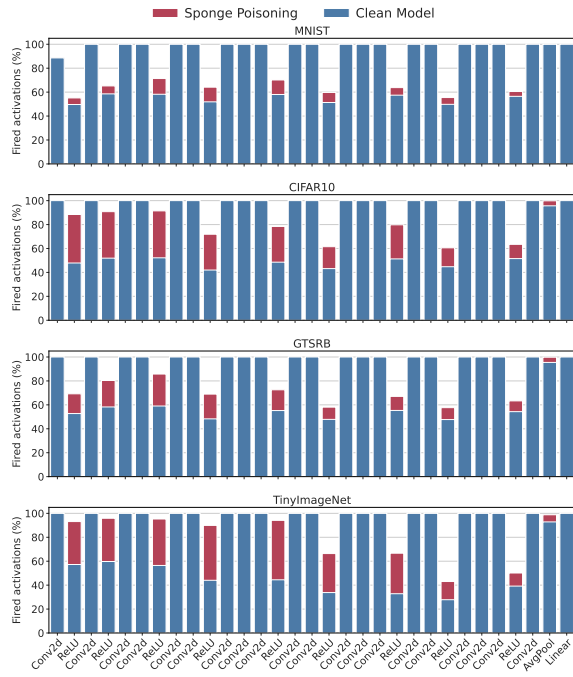


Fig. 17. The differences in the average percentage of positive activations in all layers for a clean ResNet18 model and a Sponge Poisoned ResNet18 model. The average is calculated over all images in the test set.